International Journal of Engineering Innovation & Research
Volume 3, Issue 1, ISSN: 2277 – 5668

Study of Key Theoretical and Technical Features of Dynamic Loading of High Voltage Overhead Transmission Lines

Shadreck Mpanga
School of Engineering, University of Zambia, Lusaka, Zambia 10101
Email: shadreck.mpanga@gmail.com

Ackim Zulu
School of Engineering, University of Zambia, Lusaka, Zambia 10101
Email: ackim.zulu@unza.zm

Luka Ngoyi
School of Engineering, University of Zambia, Lusaka, Zambia 10101
Email: luka.ngoyi@unza.zm

***Abstract* –This paper presents the research on the dynamic loading technology of overhead lines and its effects on the external insulation of the transmission lines. Existing literature on dynamic loading has explained the two main methods, i.e., static temperature raising and real time loading techniques, used for upgrading the transmission capacity of existing transmission lines. However, the forms of the heat balance equation used to explain these techniques in many articles may not clearly be discerned. This paper uses the form of the heat balance equation that clearly shows how the parameters in the equation lead to increased loading of the overhead lines. How the electrical parameters are related to the mechanical parameters in an overhead conductor during loading is also clearly shown. Thus, this paper shows that operation of an overhead line conductor is actually a form of an electromechanical interaction. Two critical electrical power equipment, the transformer and circuit breaker, are examined during a load flow simulation in ETAP to show how they are affected by dynamic loading.**

***Keywords* – Electromechanical Interaction, Insulation, Load Current, Numerical Simulation.**

I. INTRODUCTION

An electromechanical interaction in overhead power lines in this paper is taken to imply a situation where an agitation in mechanical properties gives rise to quantifiable electrical properties and vice versa. For instance, conductor sag is the ultimate desired parameter used to quantify the loading of overhead lines. Three safety criteria, conductor sag, temperature and stress, are actually used in the Dynamic Thermal Circuit Rating (DTCR), developed by the American Power Research Institute (EPRI), for up-rating of the transmission capacity of overhead lines [1]-[5]. The increase in conductor temperature has a large bearing on the aging and mechanical strength of the overhead power transmission lines. This also determines the insulation integrity of the line. Load current is the main cause for the heat transfer process in these power lines. In fact, high current flows can lead to overheating of the overhead conductor thereby resulting in excessive line sagging. This occurrence causes reduced electrical clearances with the inevitable effect of more electromagnetic fields being detected on the ground of the transmission circuit corridor [6].

Fig.1 is a good example where an electromechanical reaction can clearly be observed. It implies that for line lengths less than L, the transmission circuit is limited by thermal stresses whereas for lines longer than L, transmission capacity is limited by security stability. What this means is that short transmission lines have electrical and thermal stresses defining their transmission capacity, and long transmission lines have voltage stability [8] and mechanical stresses defining their transmission capacity. Thus, the mechanical properties of an overhead conductor determines its suitability for capacity upgrade through dynamic loading.

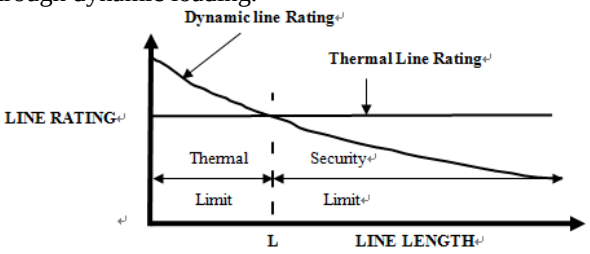

Fig.1. Dynamic and thermal rating of an overhead transmission line [7]

A number of publications [9]-[12] have quantitatively discussed these properties in detail, in some cases only giving a qualitative linkage to the electrical properties. Since it is clear that climatic loadings such as wind, ice and temperature do influence the mechanical loading of overhead lines, there is need to show, at least theoretically, how mechanical and electrical parameters connect together in appropriate mathematical models.

This paper uses the heat balance equation [1]-[5],[13] as the starting point for developing the mathematical models that bring the electromechanical reaction to the fore. It shows, mathematically, how dynamic loading of overhead lines affects sag and tension. How the short circuit capability of conductors is related to the heat transfer is also mathematically explained. Numerical simulations are then done in MATLAB to see the kind of curves that emanate from these scenarios. Load flow simulations are done in ETAP to see how the power transformer and the high voltage circuit breaker respond to increased loading of the line. The circuit breaker is used to check on the short circuit status of the conductors after the dynamic loading technology has been introduced.

II. ELECTROMECHANICAL INTERACTION IN HIGH VOLTAGE OVERHEAD LINES

A. The Heat Balance Equation for High Voltage Overhead Transmission Lines

There are various ways of writing the heat balance equation. This paper uses the form shown in (1) where $\boldsymbol{I}$ is the load current in amperes, $\boldsymbol{R_m}$ resistance in ohms per meter length, $\boldsymbol{s_a}$ solar absorption coefficient, $\boldsymbol{I_s}$ solar irradiation intensity in W/m^2, $\boldsymbol{d_m}$ conductor diameter in meters, $\boldsymbol{\Delta t}$ temperature rise in $^\circ$C above ambient, i.e. t-t_a, $\boldsymbol{p}$ air pressure in atmospheres, $\boldsymbol{v_m}$ wind velocity in m/s, $\boldsymbol{e}$ relative emissivity of conductor surface, $\boldsymbol{T}$ conductor temperature on the Kelvin scale, and $\boldsymbol{T_a}$ ambient temperature on the Kelvin scale.

$$I^2R_m + s_aI_sd_m = 18\Delta t\sqrt{pv_md_m} + 17.9ed_m\left[\left(\frac{T}{100}\right)^4 - \left(\frac{T_a}{100}\right)^4\right] \quad (1)$$

Thus, the first term on the left-hand side in (1) accounts for heating up of the conductor through ohmic losses whereas the second term accounts for heating up of the conductor through solar insolation. The first term on the right-hand side in (1) accounts for conductor heat loss through convection while the second term accounts for heat loss through radiation.

Hence, it is clear from (1) how heat transfer takes place in overhead conductors. It is one equation that enables designers to know how much heat can be dissipated by the conductor and thereby fix the current rating of the conductor.

B. Dynamic Loading Effect on Sag and Tension of Overhead Conductors

The conductor sag f for arbitrary temperatures and additional loads and/or the tensile stress for arbitrary sags and temperatures are calculated as indicated in (2), where δ_m is conductor tensile stress at temperature t_m, γ_m relative density of the conductor, l conductor span length less than 500 m long, δ_n maximum permissible tensile stress at temperature t_n, E modulus of elasticity of the conductor, γ_n relative density of the conductor with additional load, and α thermal expansion factor of the conductor.

$$\delta_n - \frac{E\gamma_n^2l^2}{24\delta_n^2} = \delta_m - \frac{E\gamma_m^2l^2}{24\delta_m^2} - \alpha E(t_n - t_m) \quad (2)$$

Now, assume that the temperature differences in (1) and (2) are equal, i.e. t_n-t_m =Δt. Thus, substituting Δt for t_n-t_m in (2) and rearranging gives (3). Sag is given as shown in (4).

$$\Delta t = \frac{\delta_m - \delta_n}{\alpha E} - \frac{l^2}{24\alpha}\left(\frac{\gamma_n^2}{\delta_n^2} - \frac{\gamma_m^2}{\delta_m^2}\right) \quad (3)$$

$$f = \frac{\gamma_m.l^2}{8\delta_m} \quad (4)$$

Equation (4) can be rearranged as l^2=8$f\delta_m/\gamma_m$ and then substituting this expression into (3), we obtain (5) below.

$$\Delta t = \frac{\delta_m - \delta_n}{\alpha E} - \frac{f\delta_m}{3\alpha\gamma_m}\left(\frac{\gamma_n^2}{\delta_n^2} - \frac{\gamma_m^2}{\delta_m^2}\right) \quad (5)$$

When (5) is substituted into (1) and then making I^2 the subject of the formula, we obtain (6) as shown below. At this stage, the effect of load current I or dynamic loading of overhead lines on conductor sag f can clearly be envisaged.

$$I^2 = 18\sqrt{p.v_m.d_m}\left[\frac{\delta_m - \delta_n}{\alpha E R_m} - \frac{f\delta_m}{3\alpha\gamma_m R_m}\left(\frac{\gamma_n^2}{\delta_n^2} - \frac{\gamma_m^2}{\delta_m^2}\right)\right] + \frac{17.9ed_m}{R_m}\left[\left(\frac{T}{100}\right)^4 - \left(\frac{T_a}{100}\right)^4\right] - \frac{s_aI_sd_m}{R_m} \quad (6)$$

Equation (6) leads to complicated partial differential equations of current with respect to conductor sag or stress, but it is easy to deduce from it that dynamic loading of overhead lines is definitely limited by conductor sag as it is directly proportional to the absolute value of the load current. The consequence of this is a reduction in conductor stress as (6) indicates. This results in increased conductor sag and the consequent reduction in overhead conductor-ground clearance. Reduced clearance in turn leads to more electromagnetic fields on the ground of the transmission line corridor.

A more realistic approach to analyzing an electromechanical reaction is to study the behavior of an overhead conductor at high temperatures. Equation (2) assumes that mechanical loads are maximum at lower temperatures. Now the following mathematical models assume that electrical loads are maximum at higher temperatures. When current flows in a conductor, there is a heat transfer process that takes place. This heat causes a conductor thermal elongation whereby its length $\boldsymbol{L}$ increases while the span length $\boldsymbol{l}$ remains the same. This implies both thermal expansion and strain under tension must be considered for sag calculation. The tension $\boldsymbol{H_0}$ of the conductor and the temperature $\boldsymbol{T_0}$ at which the conductor was strung must be specified apriori. Hence, the tension $\boldsymbol{H}$ at which the length of an elongated overhead conductor is equal to the catenary [14] conductor's length can be known for sag calculations. Equation (7) shows how to do this where $\boldsymbol{L_0}$ is initial conductor length in meters, $\boldsymbol{L}$ conductor length in meters at a high temperature $\boldsymbol{T}$, $\boldsymbol{E}$ modulus of elasticity, $\boldsymbol{A}$ conductor cross sectional area in m^2, $\boldsymbol{\varepsilon_c}$ plastic deformation due to creep, and (H-H_0)/EA accounts for elastic strain.

$$L = L_0\left[1 + \alpha_T(T - T_0)\right]\left(1 + \frac{H - H_0}{EA} + \varepsilon_c\right) \quad (7)$$

Now the linearlized form of conductor length L can also be written as given in (8) where the parameters have already been defined.

$$L = l + \frac{w^2l^3}{24H^2} \quad (8)$$

When (8) is substituted into (7), we obtain (9) below:

$$l + \frac{w^2l^3}{24H^2} = \left(l + \frac{w^2l^3}{24H_0^2}\right)\left[1 + \alpha_T(T - T_0)\right]\left(1 + \frac{H - H_0}{EA} + \varepsilon_c\right) \quad (9)$$

Equation (9) can now be solved for horizontal tension H, which can be used to calculate sag. To do that, the equation is first multiplied by H^2 on both sides and the result is as depicted in (10).

$$lH^2 + \frac{w^2l^3}{24} = H^2\left(l + \frac{w^2l^3}{24H_0^2}\right)\left[1 + \alpha_T(T - T_0)\right]\left(1 - \frac{H_0}{EA} + \varepsilon_c + \frac{H}{EA}\right) \quad (10)$$

Rearrangement and simplification of (10) leads to (11) below:

$$\left(1+\frac{w^2l^2}{24H_0^2}\right)\left[1+\alpha_T(T-T_0)\right]\left(\frac{1}{EA}\right)H^3+\left(1+\frac{w^2l^2}{24H_0^2}\right)\left[1+\alpha_T(T-T_0)\right]\left(1-\frac{H_0}{EA}+\varepsilon_c\right)H^2-H^2-\frac{w^2l^2}{24}=0 \quad (11)$$

At this stage, it is clear that (11) is a polynomial equation in the form shown in (12). Conductor sag f that results as a consequence of the electromechanical reaction can now be resolved as rewritten in (13). The heat balance equation is written again in (14) for comparison purposes.

$$a_1H^3+a_2H^2+a_3H+a_4=0 \quad (12a)$$

$$\left.\begin{aligned} a_1&=\left(1+\frac{w^2l^2}{24H_0^2}\right)\left[1+\alpha_T(T-T_0)\right]\left(\frac{1}{EA}\right)\\ a_2&=\left(1+\frac{w^2l^2}{24H_0^2}\right)\left[1+\alpha_T(T-T_0)\right]\left(1-\frac{H_0}{EA}+\varepsilon_c\right)-1\\ a_3&=0\\ a_4&=-\frac{w^2l^2}{24}\end{aligned}\right\} \quad (12b)$$

$$f=\frac{wl^2}{8H} \quad (13)$$

$$I^2R_m+s_aI_sd_m=18\Delta t\sqrt{pv_md_m}+17.9ed_m\left[\left(\frac{T}{100}\right)^4-\left(\frac{T_a}{100}\right)^4\right] \quad (14)$$

When we assume that T_0 and T_a are equal in (12) and (14), it is easy to see clearly how the electrical loads are related to the mechanical loads through the heat transfer process necessitated by a rise in conductor temperature.

C. Short Circuit Thermal Rating of Overhead Conductors

From the data provided on the short-circuit thermal withstand strength of conductors [15], it is easy to come up with a formula for the permissible short-circuit thermal rating $\boldsymbol{I_{th}}$ of overhead conductors. Equation (15) shows the formula where $\boldsymbol{A}$ is conductor cross-sectional area in m^2, $\boldsymbol{k_{20}}$ conductivity, $\boldsymbol{\alpha_{20}}$ temperature coefficient, $\boldsymbol{\delta_e}$ is permissible short circuit temperature in °C, $\boldsymbol{\delta_b}$ is temperature just before short circuit in °C, $\boldsymbol{t}$ is time in seconds, $\boldsymbol{c_{st}}$ is specific thermal capacity, and $\boldsymbol{\gamma_{sd}}$ is specific density of the conductor.

$$I_{th}=A.\frac{\sqrt{\left\{\frac{k_{20}.c_{st}.\gamma_{sd}}{\alpha_{20}}.\ln\frac{1+\alpha_{20}(\delta_e-20)}{1+\alpha_{20}(\delta_b-20)}\right\}}}{\sqrt{t}} \quad (15)$$

Two important purposes of a short circuit study on transmission lines as depicted in (15) are: (i) To know whether or not the line will be able to withstand the electromagnetic fields between the conductor and the ground. (ii) To limit the maximum conductor temperature of the extreme high current. All these points help reveal the insulation integrity of the overhead transmission line.

III. Modeling of Electromechanical Interaction Results And Analysis

A. Dynamic Capacity Increase of Overhead Lines

Using the model described by (1) for an ambient temperature of 25 °C and conductor temperature of 40 °C, wind velocity was varied from 0 to 25 m/s and fig. 2(a) shows the results where it can be deduced that current rating increases with increasing wind velocity. In fig. 2(b), ambient temperature is kept constant at 20 °C while wind velocity is kept constant at 1.5 m/s as conductor temperature was varied from 20 °C to 100 °C. The numerical simulation results indicate that current rating increases with an increasing conductor temperature too. This approach makes it possible to easily understand what happens during dynamic loading of overhead transmission lines. The conductor used is the 21.78 mm ACSR conductor at 1 atmosphere with e=0.5 and s_a =0.6.

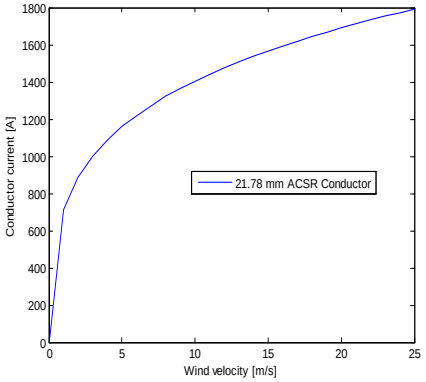

(a) Load Current Vs Wind Velocity

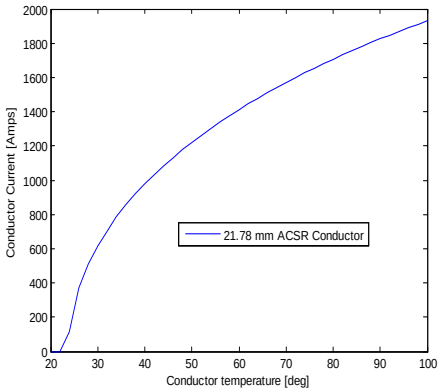

(b) Load Current Vs Conductor Temperature

Fig.2. Rating variation of a 21.78 mm ACSR overhead line conductor with climatic loadings

What fig. 2(a) demonstrates is the real-time use of weather data, whereas fig. 2(b) demonstrates the static conductor temperature raising techniques to establish an accurate dynamic rating of an overhead transmission line conductor. It is clear here that wind velocity and ambient temperature have a far greater influence on the loading of overhead conductors.

B. *Ampacity Effects on Sag and Tension*

The same conductor in fig. 2 is used to observe the load current effects on sag and tension at 1 atmosphere, 1000 W/m^2 solar insolation, 2 m/s wind speed, 0.5 emissivity and 0.6 solar irradiation constant. Equations (12) through (14) are employed this time around in MATLAB. A 125 meter span length is assumed to be originally tensioned at 20% of rated tensile strength on a 20 $^{\circ}$C day. The conductor is rated at 75 $^{\circ}$C. It is required to observe the behavior of sag and tension of the conductor at its original and rated temperatures. After 10 years, the transmission line happens to have a permanent elongation of 0.05%. Fig. 3(a) shows how load current varies with conductor temperature whereas fig. 3(b) shows how sag varies with tension.

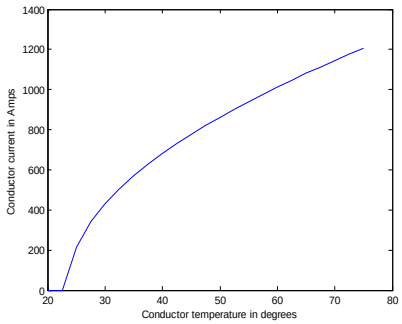

(a) Load current Vs Conductor Temperature

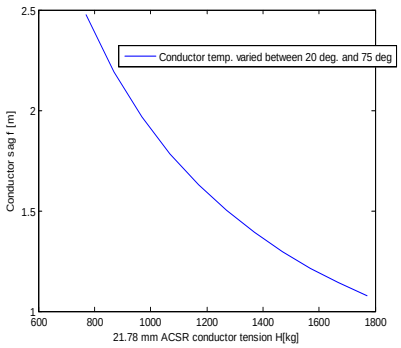

(b) Conductor sag Vs Conductor tension

Fig.3. Variation of conductor sag and tension with increase in conductor temperature

These results indicate that as load current increases, conductor sag also increases. This translates to a corresponding reduction in conductor tension at higher temperatures. Conductor sag was calculated as 1.08 m at 20 $^{\circ}$C while conductor tension was calculated as 1769 kg. When conductor temperature increased to 75 $^{\circ}$C, conductor sag was calculated as 2.38 m while conductor tension dropped to 780 kg.

It must be noted that in dynamic simulations, the long-term issues such as conductor heating and sagging, that take several minutes are not easy to model. In fact, they have tens of minutes of time constant. Thus, the manner in which the modeling has been done in this paper helps to appreciate the behavior of conductor sag with change of load current.

C. *Short Circuit Thermal Ratings of Conductors*

Taking a 484.5 mm^2 ACSR conductor as an example, and assuming short circuit duration of 1 second, a maximum operating conductor temperature of 75 $^{\circ}$C and a short circuit temperature of 200 $^{\circ}$C, a short circuit curve produced is as shown in fig. 4(a) when the parameters are applied in (15). Only the Aluminum area was considered in this case, and the short circuit current has the highest value of 116.2 kA, attenuating to 36.8 kA 1 second later. Currents of these magnitudes can damage overhead line insulation due to extra heat generated, burn support insulators, cause instability and sagging of the conductors due to thermal expansion.

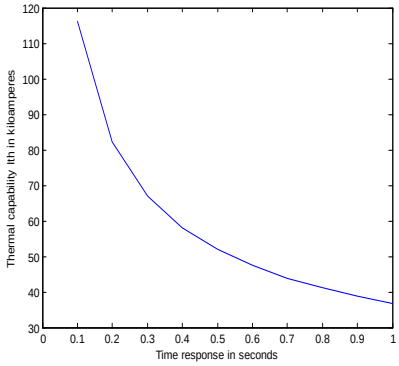

(a) Curve at 75 $^{\circ}$C

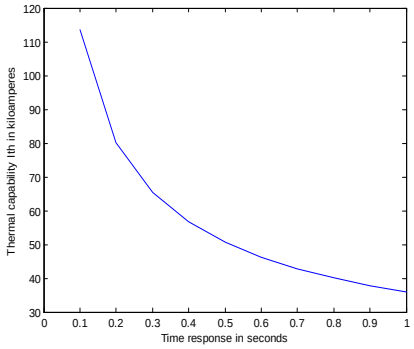

(b) Curve at 80 $^{\circ}$C

Fig.4. Short-circuit curves for a 484.5 mm^2 conductor due to temperature variations

However, with modern high speed microprocessor relays able to pick up and send the fault signal to the circuit breaker in about 10 ms, it is extremely rare for a fault to last 1 second in high voltage transmission systems, even 0.1 s is rare. Conductor thermal withstand ratings have been used in fig. 4(a), actual short circuit current values are expected to be smaller depending on the configuration of the overhead line.

To check on how the short circuit current changes when the conductor temperature increases, the conductor temperature was changed from 75 $^{\circ}$C to 80 $^{\circ}$C, keeping the short circuit temperature at 200 $^{\circ}$C, and the result is as shown in fig. 4(b). The maximum short circuit current value slightly reduces to 113.4 kA, and attenuating to 36 kA in 1 second. This is expected since conductor resistance increases with increasing conductor temperature.

International Journal of Engineering Innovation & Research
Volume 3, Issue 1, ISSN: 2277 – 5668

Nevertheless, conventional simulations of short circuit analysis in a software like ETAP (see section 3D) indicate that the maximum short circuit value does not change regardless of what happens to the loading of the overhead line conductors. The values obtained in fig. 4 do not seem to disagree with that fact. The above numerical simulations were done in order to gain at least a fundamental understanding and appreciation of the technicalities confronted with the electromechanically loading of the overhead transmission lines.

D. Load Flow Studies in ETAP

The ETAP software as shown in fig. 5 was used for the load flow and short circuit analysis during dynamic loading studies. The ETAP transmission line editor is a powerful tool for varying line parameters and seeing how they affect the loading of the overhead lines. The parameters used in the case study were entered as shown in fig. 5 where it can clearly be seen that all the important features of a line such as sag and tension, conductor ampacities, diameter, temperature, height, spacing and wind velocity can easily be studied. The transmission line in fig. 5 comes from a utility network with a short circuit capacity of 30,000 MVA and feeds a lumped dynamic load that was varied from 600 MVA to 745 MVA via a 500/33 kV Transformer.

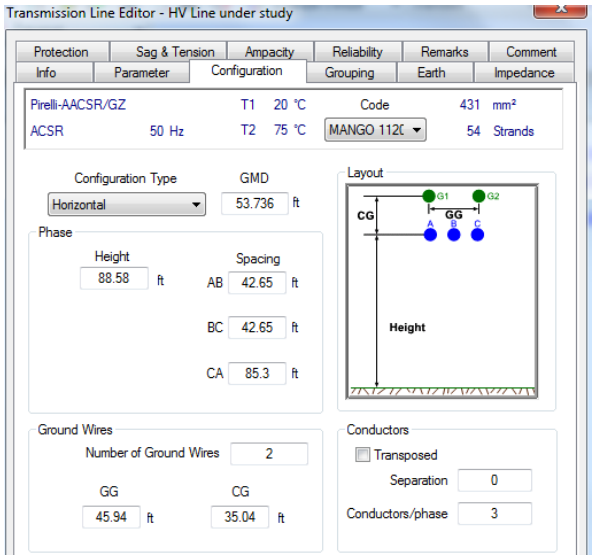

Fig.5. Entering of case study parameters into ETAP software for dynamic loading studies

High voltage overhead transmission lines are usually long in expanse. To make dynamic loading possible, the line must be subjected to capacitive compensation to prevent too much voltage drop along the line since, when line current is increased, voltage drop will also increase. To demonstrate the principle, line compensation is done at the end section of a 200 km long line. This is as shown in fig. 6 from Bus 4 to Bus 5 with compensation capacitor, *V. comp. capacitor*. With a load of 600 MVA, the simulated results appear as shown in fig. 6.

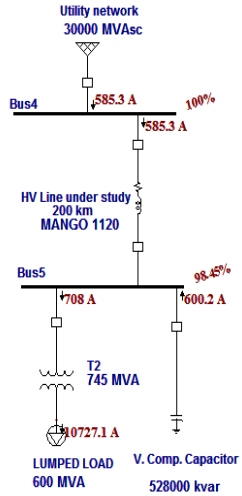

(a) Load flow study

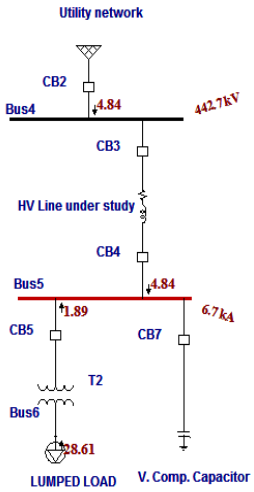

(b) Short circuit study in HV line

Fig.6. ETAP Simulation of a dynamic load (600 MVA)

When the load was increased to 700 MVA, the results are as depicted in fig. 7, and fig. 8 is for a 745 MVA load.

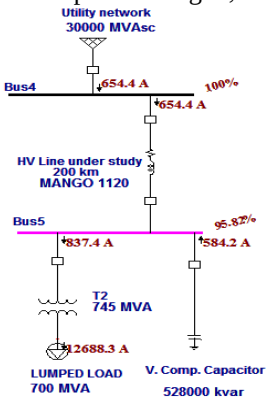

(a) Load flow study in alert state

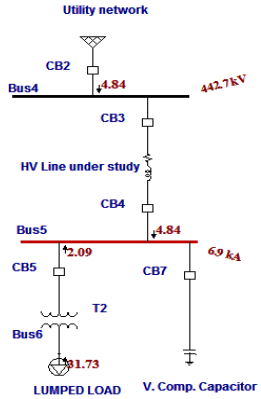

(b) Short circuit study in HV line

Fig.7. ETAP Simulation of a dynamic load (700 MVA)

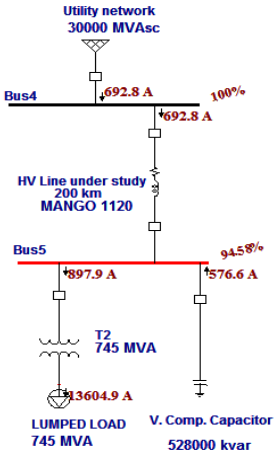

(a) Load flow study in collapse state

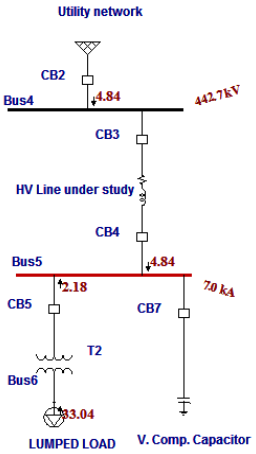

(b) Short circuit study in HV line

Fig.8. ETAP Simulation of a dynamic load (745 MVA)

From the above ETAP simulations, it can be concluded that;

(i) When the load is increased, voltage drop at the end section of the line is more pronounced, and there is an alert warning if the percentage of voltage drops close to 95%. This is the situation experienced in fig. 7 (a) at Bus 5 in purple colour.
(ii) From point (i) above, it follows that before dynamic loading is implemented, a transmission line has to be compensated if this has not happened already.
(iii) For an existing compensated transmission line, there might be a need to uprate the existing compensation equipment. The rating and cooling systems in place for the power transformers in the transmission circuit must also be checked. This is because increasing the loading will increase the temperature gradients within the transformer, and a point will be reached where these gradients will limit the ability to increase the load any further. The solution may be to improve the cooling mechanism of the power Transformer, depending on its manufacture.
(iv) The short circuit current in the high voltage line of fig. 6-fig. 8 is constant at 4.84 kA regardless of the loading levels of the conductors.
(v) The short circuit current cleared by the HV breaker CB2 is also constant at 35.33 kA regardless of whether the fault happens at Bus 4 or Bus 5.
(vi) Once the operating voltage drops below 95% of nominal voltage of 500 kV, the undervoltage relays trip the breakers.

IV. Conclusion

This paper has explained the intricate relationship between the electrical loading and the mechanical design of high voltage overhead transmission lines. It has been shown that successful operation of a high voltage overhead transmission power line depends to a large extent on the mechanical design of its structures. Case studies have been applied on the derived relationships and the results from the predictions appear to be a realistic expectation of what occurs in the power system equipment. The mechanical strength must come with the protection against the most probable weather conditions, some of which in turn result in increased electrical loading of the line.

Acknowledgment

Mr. Shadreck Mpanga, Dr Ackim Zulu, and Dr Luka Ngoyi would like to acknowledge with thanks the support rendered by The University of Zambia via the school of engineering towards the successful completion of this paper.

References

[1] Dale A. Douglass, Daniel C. Lawry, Abdel-Aty Edris, and Earle C. Bascom, "Dynamic Thermal Ratings Realize Circuit Load Limits," *IEEE Computer Applications in Power*, 2000, pp. 39-44.

[2] Dale A. Douglass, and Abdel-Aty Edris, "Field Studies of Dynamic Thermal Rating Methods for Overhead Lines," *IEEE Transactions on Power Delivery*, 1999, pp. 842-851.

[3] Dale A. Douglass, Abdel-Aty Edris, and Glenn A. Pritchard, "Field Application of a Dynamic Thermal Circuit Rating Method," *IEEE Transaction on Power Delivery*, 1997, 12(2), pp. 823-831.

[4] Dale A. Douglass, and Abdel-Aty Edris, "Real Time Monitoring and Dynamic Thermal Rating of Power Transmission Circuits," *IEEE Transactions on Power Delivery*, 1996, 11(3), pp. 1407-1418.

[5] Dave Roberts, Philip Taylor, and Andrea Michiori, "Dynamic Thermal Rating for Increasing Network Capacity and Delaying Network Reinforcements," *CIRED Seminar: Smart Grids for Distribution*, 2008, (3), pp. 1-4.

[6] Shadreck Mpanga, Wang Feng, and Chen Chun, "Electromagnetic Field Evaluation of a 500 kV High Voltage Overhead Line," *TELKOMNIKA*, 2013, 11(2), pp. 789-796.

[7] K. E. Holbert, and G. T. Heydt, "Prospects for Dynamic Transmission Circuit Ratings," *The Institute of Electrical and Electronic Engineers*, 2001, pp. 205-208.

[8] D. Harikrishna, and N. V. Srikanth, "Dynamic Stability Enhancement of Power Systems Using Neural-Network Controlled Static-Compensator," *TELKOMNIKA*, 2010, 10(1), pp. 9-16.

[9] Jerry M. Hesterlee, Eugene T. Sanders, and Frank R. Thrash, Jr., "Bare Overhead Transmission and Distribution Conductor Design Overview," *IEEE Transactions on Industry Applications*, 1996, 32(3), pp. 709-713.

[10] J. Bradburg, G.F. Kuska, and D.J. Tarr, "Sag and Tension Calculations for Mountainous Terrain," *IEEE PROCEEDINGS*, 1982, 129(5), pp. 213-220.

[11] Shelley L. Chen, W. Z. Black, and Michael L. Fancher, "High-Temperature Sag Model for Overhead Conductors," *IEEE Transactions on Power Delivery*, 2003, 18(1), pp. 183-188.

[12] Liu Yongfu, Zhang Liguo, and Wang Jun, "Computation of Standard Sag of Overhead Lines for Power Grid Based on Mathematical Model of Iterative Technique," *International Conference on Computer Engineering and Technology*, 2010, 1(2), pp. 445-448.

[13] Rakosh Das Begamudre, *Extra High Voltage AC Transmission Engineering*, 3rd edition, New Delhi: New Age International (P) ltd, 2006, pp. 1-405.

[14] Mottis Y., *et al*, "Limitations of the Ruling Span Method for Overhead Line Conductors at High Temperatures," *IEEE Transactions on Power Delivery*, 1999, 14(2).

[15] Juergen Schlabbach, and Karl-Heinz Rofalski, *Power System Engineering*, Germany, Weinheim: WILEY-VCH Verlag GmbH & Co. KGaA, 2008, pp. 137-157.

Author's Profile

Mr. Shadreck Mpanga

obtained his Bachelor of engineering degree in electrical and electronic engineering from The University of Zambia, Lusaka, Zambia, in 2004. He obtained his Master of engineering degree in electrical engineering from Hunan University, China, in 2013.

He published one paper during his Master's studies. He is currently working for The University of Zambia in the department of electrical and electronic engineering. His research interests are in high voltage and insulation technology, and power systems.

Dr. Ackim Zulu

received the B.Eng. degree in electrical engineering from the University of Zambia, Lusaka, Zambia, in 1992, the M.Sc. degree in electrical power engineering from Heriot-Watt University, Edinburgh, U.K., in 1994, and the Ph.D. degree from Newcastle University, Newcastle upon Tyne, U.K., in 2010.

He has been a Lecturer at the University of Zambia since 1994. His research is in multidisciplinary areas involving electrical power engineering.

Dr. Luka Ngoyi

holds a Doctorate from Virginia Polytechnic and State University, USA and a Masters degree in electric power systems and networks from St. Petersburg State Polytechnic University, Russia. Currently, he is teaching at the University of Zambia in the Department of Electrical and Electronic engineering, where he has served for more than 10 years.
His research interests are in electric circuits and power systems.